

RESEARCH

Open Access



A simple ANN-MLP model for estimating 60-GHz PDP inside public and private vehicles

Rajeev Shukla^{1*} , Abhishek Narayan Sarkar¹, Aniruddha Chandra¹, Jan M. Kelner², Cezary Ziolkowski², Tomas Mikulasek³ and Ales Prokes³

*Correspondence:
rajeev2504s@gmail.com

¹ ECE Department, National Institute of Technology, M. G. Avenue, Durgapur 713209, India

² Institute of Communications Systems, Faculty of Electronics, Military University of Technology, 00908 Warsaw, Poland

³ Department of Radio Electronics, Brno University of Technology, 61600 Brno, Czech Republic

Abstract

Radio wave propagation in an intra-vehicular (IV) environment is markedly different from other well-studied indoor scenarios, such as an office or a factory floor. While millimetre wave (mmWave)-based intra-vehicular communications promise large bandwidth and can achieve ultra-high data rates with lower latency, exploiting the advantages of mmWave communications largely relies on adequately characterising the propagation channel. Channel characterisation is most accurately done through an extensive channel sounding, but due to hardware and environmental constraints, it is impractical to test channel conditions for all possible transmitter and receiver locations. Artificial neural network (ANN)-based channel sounding can overcome this impediment by learning and estimating the channel parameters from the channel environment. We estimate the power delay profile in intra-vehicular public and private vehicle scenarios with a high accuracy using a simple feedforward multi-layer perception-based ANN model. Such artificially generated models can help extrapolate other relevant scenarios for which measurement data are unavailable. The proposed model efficiently matches the taped delay line samples obtained from real-world data, as shown by goodness-of-fit parameters and confusion matrices.

Keywords: Channel sounding, Intra-vehicular communication, Millimetre wave, Multilayer perceptron, Power delay profile

1 Introduction

Recent market research from Wireless Watch [1, 2] predicts a threefold increase in the wireless intra-car connections market, from 279.3 million in 2022 to a whopping 828.7 million in 2030. When we consider large public commuter vehicles (bus, trolleybus, tram etc.) along with the small private vehicles, the figures would be even more startling. No wonder there has been a surge of startups in the domain, and both industry and academia are interested in wireless intra-vehicular communication (IVC) research.

With technological advancement and the increase in the consumer-friendly market, the number of features and technologies incorporated inside a vehicle has increased considerably. Wired IVC connections between different vehicular communication modules get cumbersome, raising design, manufacturing, and installation issues. Inversely, wireless IVC systems have high-speed duplex data links, which are better equipped to

handle multiple tasks through one system, thus providing more convenience, a simplified design, and hassle-free installation. The significance of wireless IVC can be estimated by understanding various savings introduced due to the reduction in the number of wires. Approximately five miles of wires is used in modern-day vehicles for connection between different nodes of IVC [3]. Cutting the use of wires reduces the mass of the vehicles by at least 40 kg. This incorporates cost savings on manufacturing, assembly, warranty, and maintenance. Further, a reduction in weight increases fuel efficiency. Additionally, a wireless harness means the flexibility of inclusion of newer technologies to increase security and enhance safety protocols, better automation, and user experience [4].

The major functions of wireless IVCs include assisting in signalling and controlling operations, passenger assistance, Heat Ventilation and Air-Conditioning (HVAC) control, video surveillance in public vehicles, infotainment services, and many more. To perform these operations smoothly, a knowledge of the wireless channel environment plays an important role. In addition to these facts, today's communication era empowers its users with on-the-move connectivity to utilise their time on their mobile devices using various platforms like gaming, media, entertainment, and infotainment. With the introduction of 5 G wireless networks, these platforms will be more engaging. All these add to the exponential increase in the demand for on-demand high data rates for various data network services [5]. Adequate information on the radio channel plays a critical role in achieving such a high data rate.

Modern wireless IVCs are data-intensive, meaning wireless IVCs require the system to have high data handling capacity, a data rate in giga bits per second (gbps), low latency, and large bandwidth. Bandwidth in existing sub-6 GHz systems is not enough to handle large amounts of data. Bluetooth and Zigbee-based systems have major latency, reliability, and security issues, whereas ultrawideband (UWB) cannot provide data rate in the gbps order. The millimetre wave (mmWave) spectrum is under-utilised, and properties like large bandwidth, high data rate, and low latency offer an adequate solution. MmWave spectrum orthodoxly spans from 30 to 300 GHz, which means GHz contiguous frequency bands are available to exploit, leading towards Gbps data rate without incorporating complex spectrally efficient hardware in the transmitter or receiver side.

IVC channels operating at mmWave bands are quite different from conventional cellular channels. Thus, the knowledge and understanding of pre-existing cellular channel models cannot be directly applied to the mmWave IVC channel models. Demanding time constraints, a large number of scatterers, lack of line-of-sight propagation, and human blockage make the mmWave IVC channel environment more complex. The emergence of automatic vehicles demands such models to be highly accurate and time efficient. Emulating such complex channel scenarios requires a detailed understanding of channel behaviour.

1.1 Motivation

To guarantee optimal system performance, designing of the system must be accurate and trustworthy. The channel model assists the engineers by making channel parameters readily available even for unknown scenarios. Accurate channel models ensure that

the channel parameters are close to the real-time measurements. Thus, it is necessary to develop reliable, efficient, and accurate channel models.

Channel models identify the relationship between channel parameters and the physical channel environment. It can be classified broadly into three categories. First, the statistical models are stochastic channel models with heuristically derived mathematical formulas based on massive empirical observations [6]. Such models lack preciseness, are unable to explain channel behaviour, and are computationally complex. Also, stochastic channel models are inefficient in corresponding to changes in the channel environment. The second is geometric modelling, which employs geometric information about the channel to determine the channel behaviour for a given set of T_X-R_X positions. Such models are more accurate in depicting the channel behaviour but require more computational time, are site specific, and require relevant expertise. Moreover, small changes in the channel environment mean a rerun of the entire simulation.

Both the above models mathematically characterise the multipath components (MPCs) based on some stochastic process or mathematical derivation. Both methods require extensive measurement of campaign data for the application scenario to generate the respective channel model. Measurement data may not be available for the scenario, which leads to imperfect channel models. Moreover, not every data point can be measured. To summarise, the conventional methods are not *generalisable* to any unknown channel environment for the system.

As an alternate solution to the problems of conventional channel modelling, machine learning(ml)-based channel prediction/estimation can be the ultimate solution. ML-based prediction is well documented for high accuracy. ML algorithms can learn channel parameters from the underlying channel measurement data, and the trained model can be used for channel characterisation/modelling or prediction. The research community emphasised using an ANN-based ML model for channel modelling.

1.2 Contributions

The contribution of this article is to show that a simple feedforward MLP-based ANN model can be constructed to capture the major features of a channel-sounding dataset. The test case that we considered is an intra-vehicular communication channel inside a bus and inside a car, and our operating frequency is in the 60 GHz millimetre wave range. Specifically, our contributions are as follows:

- We propose an ANN approach to synthetically generate a power delay profile (PDP) in a direct and indirect manner, which can be readily used for characterising intra-vehicular mmWave propagation.
- We derived a tapped delay-line (TDL) channel model from the synthetically generated PDPs. Different error measures show that the simulated model tallies well with the TDL model directly obtained by sampling the measured PDP.
- We compared the real-world dataset with the synthetic dataset in terms of sensitivity and goodness of fit measures.

1.3 Literature survey

Since the last decade, researchers have shown considerable interest in the field of IVC. The advancements in integrated circuit technology, efforts to make travel safer and more convenient, and increasing demand for on-the-go connectivity have fuelled the search for better solutions. Channel characterisation plays a pivotal role in developing a high-performance IVC system. A good number of literature dealt with intra-vehicular (iv) channel characterisation in public vehicles. In [7], authors provided insight into the channel environment in the 5-GHz bands inside an aircraft. The authors designed the channel model by using the root mean square error (rmse) delay spread and coherence bandwidth. Trains are one of the primary public transport vehicles, but train wagons still lack high-capacity wireless networks. In [8, 9], authors measured and analysed the intra-wagon channel in the 25–40-GHz band and the 60-GHz and 300-GHz bands using the ray tracing (rt) tool. An underground convoy was used for intra-wagon frequency-domain measurements in the 26-, 28-, and 38-GHz bands [10]. The authors concluded that antenna position and scattering-rich environment are essential in intra-wagon scenarios. The authors also advocated that the waveguide effect and human blockage affect the channel measurements and must be considered while designing the model. In another intra-wagon channel measurement campaign, authors [11] compared the channel-sounding data with RT in the 300-GHz band. Another extensively used public vehicle anywhere around the world is the bus. In [12], Semkin et al. constructed a logarithmic, distance-based pathloss model for wearable deployments inside a bus in a 60-GHz band. For the same 60-GHz band, Chandra et al. reported frequency-domain measurements inside the bus. Here, the authors [5, 13, 14] proposed PDP-based analytical model for mmWave intra-bus wireless channel. Apart from public vehicles, private vehicles like cars and SUVs are the most extensively researched. With the evolution of human-driven to driverless cars and fossil fuel-based to electric vehicles, manufacturers and researchers are working in tandem to provide better safety and the best user experience. In [15], authors developed a comprehensive simulation framework to estimate frequency-domain channel transfer function in the intra-car scenario for the UWB band. In a similar attempt, authors in [16] concluded that for UWB band intra-car scenarios, the cluster arrival rate is higher than that of indoor propagation. In contrast, the cluster decay rate is lower than the indoor propagation scenarios. The following articles [17–21] compared the performance of intra-vehicular schemes for UWB and mmWave bands. In [20], analysed the time of arrival of the packets and concluded that in the absence of human blockage, ranging accuracy is similar in both bands, but in the presence of passengers, ranging accuracy got reduced for the mmWave band, whereas [17, 18] advocated that the 60-GHz mmWave band performs better than UWB in the intra-car scenario. Authors in the intra-vehicular studies are still running; it is proved that mmWave-based channel characterisation performs better than UWB. Also, the studies are predominantly specific vehicle dependent and cannot be extended to new scenarios.

Machine learning is expected to extract channel characteristics and design and estimate a channel model much better than conventional methods. An overview of the ML-based framework for channel characterisation and modelling was provided in [22]. The article advocated the use of reinforcement learning for channel modelling in autonomous vehicles and further emphasised searching for more generalisable schemes. Indoor

channel sounding at 100 GHz was analysed by [23]. The authors proposed fingerprint-based feature extraction from PDP and then the application of various ML algorithms to design a channel model. A hybrid approach of physics based and data driven to generalise the site-specific through-vegetation scenarios was proposed in [24]. The authors proved that ML could estimate the complex mmWave channel parameters accurately based on the channel geometric configurations and T_X-R_X positions. In the articles [25–29], the authors elaborated on the use of ML in other application domains justifying the use of ML-based schemes in mmWave channel characterisation and channel modelling. In the articles [6, 30], the authors provided an extensive survey for the application of ANN-based artificial intelligence in channel characterisation and channel modelling. The authors in [31–33] provided a step-by-step tutorial for optimising the neural network followed by the application of MLP-based ANN and convolutional neural network to extract channel characteristics and used the trained model for channel modelling.

The use of artificial intelligence and machine learning (AI/ML) techniques in the context of vehicular networking is relatively recent concepts. In [34], the authors vouched for combining AI and blockchain to realise a mobile-edge-platooning cloud platform. Advanced ML techniques, such as deep reinforcement learning (DRL) and long short-term memory (LSTM), have been successfully applied in [35] and [36], respectively. Although advanced AI/ML techniques yield better results, the trade-off is the complexity, implementation time and real-time operation. In our work, we used a simple feedforward ANN-based multilayer perceptron instead and showed that considerable accuracy could also be achieved with such an introductory model.

2 Field test

An extensive 60-GHz intra-vehicular measurement campaign was carried out by the current authors at Brno University, Czech Republic, and reported in [5, 13, 14]. As illustrated in Figs. 1 and 2, the channel measurement campaign aims to provide a channel model that can enable the commuting public with onboard gigabyte wireless networks using a common vehicular access-point (ap) inside the vehicle, wirelessly connected to the roadside units or base stations through the vehicle-to-infrastructure (v2i) mobile networks. The AP will act as a transceiver and connects the passenger devices to the outside world, giving access to various on-demand high-data-rate services over static intra-vehicular channels.

2.1 Measurement campaign inside bus

Here the experimental set-up consists of an analog signal generator (model: Agilent E8257D), a scalar signal analyser (model: Rohde and Schwarz FSUP50), a pair of mmWave antennas, a power amplifier (PA), a mixer, a DC power supply, adapters, and connecting cables (Fig. 1). The signal generator sweeps all the frequencies from 55 to 65 GHz with a step size of 10 MHz generating 1001 readings in each sweep in the transmitter section. The generator output power is set to 13 dBm. The output signal is carried through a 2.5m-long phase-stable coaxial cable (model: MegaPhase TM67) to the power amplifier (model: Quinstar QPW 50662330) through standard 1.85 mm adapters. The power amplifier has a gain of 31 dBm, which is high enough to compensate for the cable loss and boosts the signal fed to the open-waveguide antenna (OWGA). A DC power

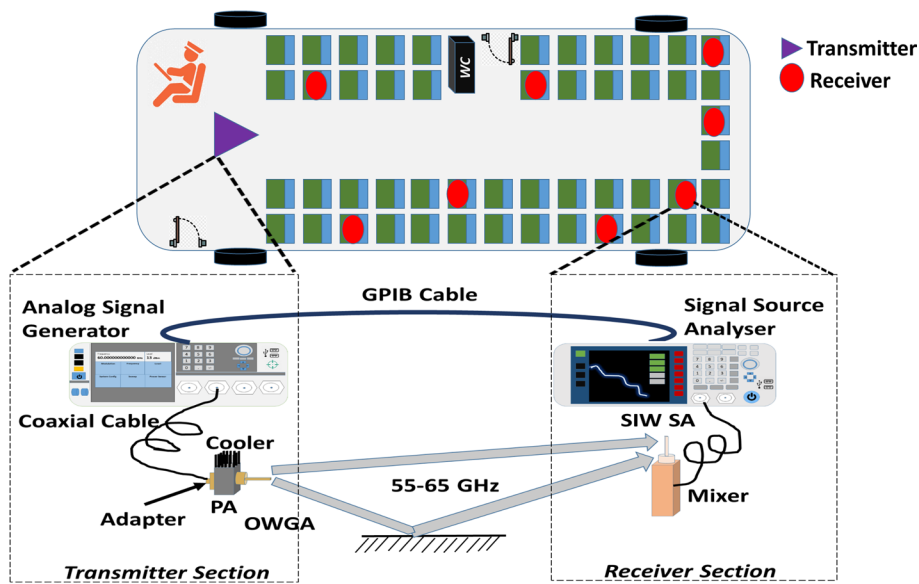


Fig. 1 Experimental set-up for bus measurement campaign

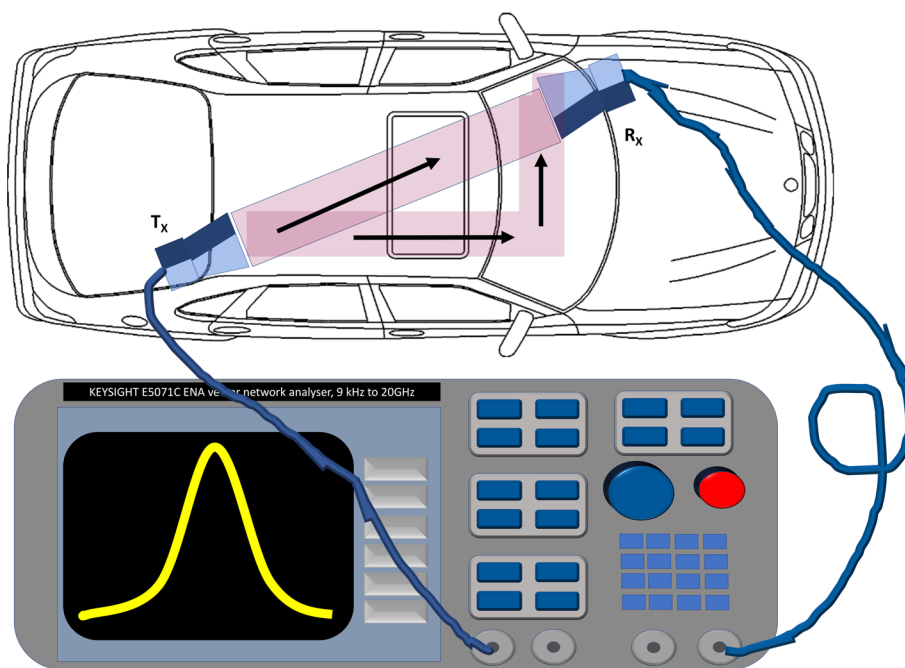


Fig. 2 Experimental set-up for car measurement campaign

supply powers the power amplifier and its accessories. A substrate-integrated waveguide slot antenna (SIW SA) intercepts the signal and sends the received signal to the signal analyser at the receiving end. An external mixer converts the signal to an intermediate frequency and helps avoid high cable loss at mmWave frequencies. The GPIB cables connect the two pieces of hardware at the transmitting and receiving sections for synchronisation. To extend the Tx and Rx distance, we can cascade several GPIB cables together.

The measurement set-up is placed inside a 50-seater Mercedes Benz Turismo bus to conduct the measurement experiments. Placing the transmitter near the ceiling at the bus's front end creates a real-time scenario, and the receiver is placed in the seat's drop-down tray to imitate a hand-held device. The receiver location was changed to different seats to cover the entire interior space of the bus in the presence/absence of passengers.

2.2 Measurement campaign inside car

Intra-car measurement set-up consists of Rohde & Schwarz ZVA67 4-port vector network analyser (VNA) with a continuous sweep capability from 110 MHz to 110 GHz, PA, pair of mmWave waveguide antennas, Fig. 2. Phase-stable coaxial cables connect the VNA to antennas. To compensate for any loss due to cable loss and to boost the dynamic range of measurements, Quinstar PA, with a 30 dB gain, was used. The losses were well-calibrated for zero transmission. A medium-sized 4-seater Skoda Octavia carries the entire set-up inside it. For a given arrangement of T_X and R_X , the forward transmission coefficient s_{21} is recorded for the frequency range of 55–65 GHz.

3 Estimating PDP with MLP

Conventional channel sounding procedures have little knowledge about the underlying channel conditions and cannot interpolate or extrapolate the data. This limits them from working in all kinds of complex channel environments [6]. The state-of-the-art studies suggest that ANN, due to its low complexity and off-line training process, is the most prominent method for implementing ML. A multilayer perceptron (MLP) is a fully connected feed-forward artificial neural network. As mentioned in [6, 30, 37], a 3-layer MLP can be an excellent choice to approximate the channel behaviour using physical parameters to a desired accuracy. Combining the MLP model with the channel environment measurement database promises estimation close to theoretical calculations. On the other hand, changing the input parameters signifies the channel environment's role in signal propagation. Simple MLP models also mean less computational complexity and less time consumption at the cost of a slight reduction in accuracy. It further reduces the need for robust, expensive computers, which reduces carbon footprints.

ANN constitutes one input layer, one output layer, and at least one hidden layer. More hidden layers or more neurons in the hidden layer usually reflect better accuracy. But when the datasets are limited, adding depth to ANN may overfit the model resulting in inaccurate predictions. To gain the 'generalisable' edge over the conventional channel models, ANN algorithms must be able to learn from the physical channel environment. To reduce the classical dichotomy between computational efficiency and accuracy selection of input parameters, precise and compact training datasets and constructing efficient ANN models are critical [32, 33]. For the current work, we chose the frequency and distance parameters as input vectors since these parameters are the most basic features for signal propagation. To increase the computational efficiency, we regularise the model by reducing the error between training and validation datasets before the model starts overfitting.

This article aims to estimate PDP using a feed-forward ANN-based MLP model with minimal physical inputs using direct or indirect processes. In the indirect method, using channel measurement data, the channel transfer function (CTF) is estimated

and estimated CTF values are used to generate PDP. In the more direct method, measurement data are first used to extract the delay spread feature for a given set of $T_x - R_x$ positions.

3.1 Indirect method

In the indirect method, physical channel features are first selected from measurement campaign datasets, as shown in Fig. 3. For this article, signal frequency spectrum (55–65 GHz with 60 GHz as centre frequency) and T_x-R_x positions are selected as input parameters as seen in the second block from left. Again from the measurement campaign data, we chose channel transfer function (CTF) corresponding to different T_x-R_x distances for the 60-GHz band as the output vector. As the data for the presence of passengers and their seat positions were insufficient, these parameters were not chosen. Using the input parameters, the MLP model is first optimised for the number of neurons using the training dataset (bottom left). Next, the optimised MLP model is trained using the training datasets, and the results are validated, as shown in the middle blocks on the right side of Fig. 3. The trained model then estimates CTFs for the given frequency spectrum. The estimated CTFs and measured CTFs are then converted from the frequency domain to the time domain using inverse fast Fourier (ifft) to generate PDP data. The simulated CTFs generate a PDP trend which is analysed and compared with PDP generated from measured test data.

3.2 Direct method

In the direct method, physical channel parameters from the measurement campaign are used to extract time delay spread data (Fig. 4). The delay spread data and the T_x-R_x positions constitute the input parameters for the training datasets. PDP sequence data extracted from CTF data from the measurement data describe the output vector. The input and output vectors are used to optimise the MLP network (bottom right block in Fig. 4) Optimised MLP network is then trained to estimate PDP for the extracted input parameters and output vector. The trained model is then fed with test data to estimate

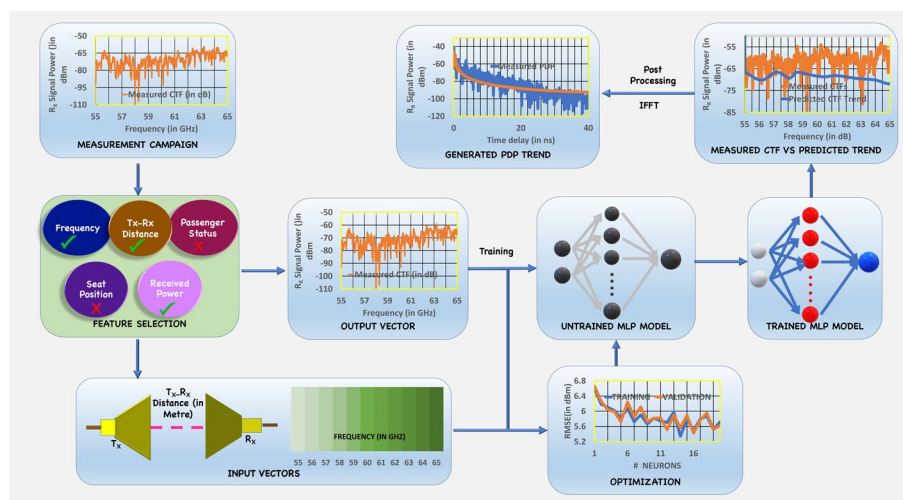


Fig. 3 Schematic for indirect PDP generation

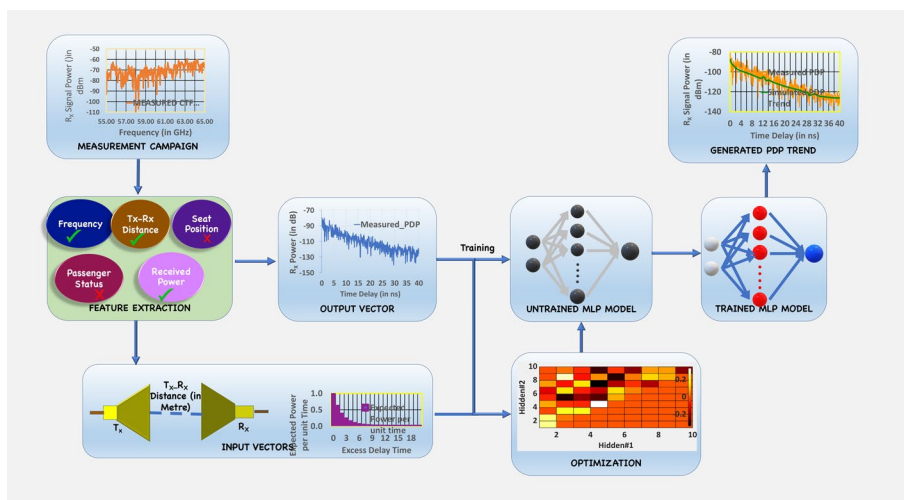


Fig. 4 Schematic for direct PDP generation

the PDP trend. The synthetic PDP trend is then compared with the PDP sequence generated from measured test data and analysed as shown in the top right block of Fig. 4.

3.3 Neuron optimisation

The choice of the number of hidden layers and the number of neurons in each hidden layer decides the accuracy of the MLP model. Anything less than the optimised value causes an under-fitting and inaccurate perception of the physical channel. Also, increasing the number of hidden layers by increasing the number of neurons increases model complexity and training time without significantly increasing the model accuracy.

In the present article, the training dataset is fed into the untrained MLP network, and the model is evaluated for different numbers of neurons in terms of the validation RMSE. The MLP architecture for which RMSE is the smallest is chosen for the final MLP model.

4 Results and discussions

The present article implements a fully connected feed-forward artificial MLP neural network. We utilised the car and bus channel sounding measurement campaign data for the current study. The dataset contains the frequency-domain CTF values for the 55–65 GHz frequency range. We tried to generate the PDP for a given set of frequency vectors and $T_x - R_x$ position vector. As explained in Figs. 3 and 4, we followed two methods for generating the synthetic PDP. Firstly, the indirect method used physical parameters like available frequency spectrum and $T_x - R_x$ position. In the second method, we converted frequency-domain CTF to time-domain CIR to generate delay spread data. Using these fabricated data, we estimate the PDP at a given distance from the receiver.

4.1 Simulation results

Our study used the ANN model to replicate the behaviour of a physical intra-vehicular wireless channel over a 55–65 GHz frequency band. We used a 3-layer MLP model to imitate the wireless channel environment inside a car and a 4-layer MLP model inside a bus. The choice for a more complex MLP model for the bus is due to the complex

channel environment, resulting in more significant multipath propagation. We observed that only a few channel parameters are required to reproduce the channel environment. Additional parameters increase the accuracy by a small margin at the cost of higher computational complexity and processing time.

Our first method utilised the frequency band information and $T_x - R_x$ position information to generate synthetic CTF data. We further observed that the obtained CTF trend roughly follows the measured CTF trend. As shown in Fig. 5, adding a small dc offset can result in the synthetic CTF trend following the measured CTF more closely. When these synthetic CTF data are used to generate the PDP sequence by applying IFFT, the resultant synthetic PDP sequence also follows the trend of the measured PDP sequence. Again here also, an additional DC offset is required.

Instead of selecting the frequency parameter and distance vector directly, implementing IFFT operation on frequency-domain data to extract the time-domain data provides improved results. As shown in Fig. 6, the synthetic PDP trend closely follows the measured PDP trend. The artificial PDP trend generates tapped delay line (TDL) model for bit-error simulations.

4.2 Tapped delay line analysis

Since the dense physical environment inside a bus gives rise to highly clustered wireless channels resulting in distinctive multipaths, TDL models allow differentiating between these scattered multipath components, with each tap representing a single component.

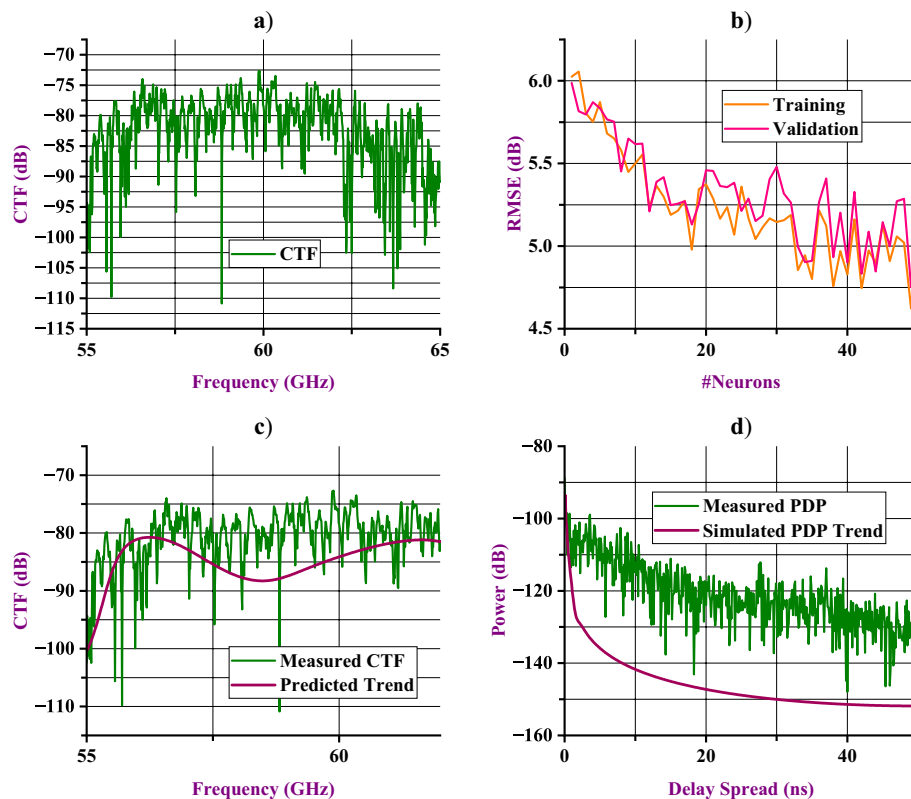


Fig. 5 Indirect generation of PDP sequence

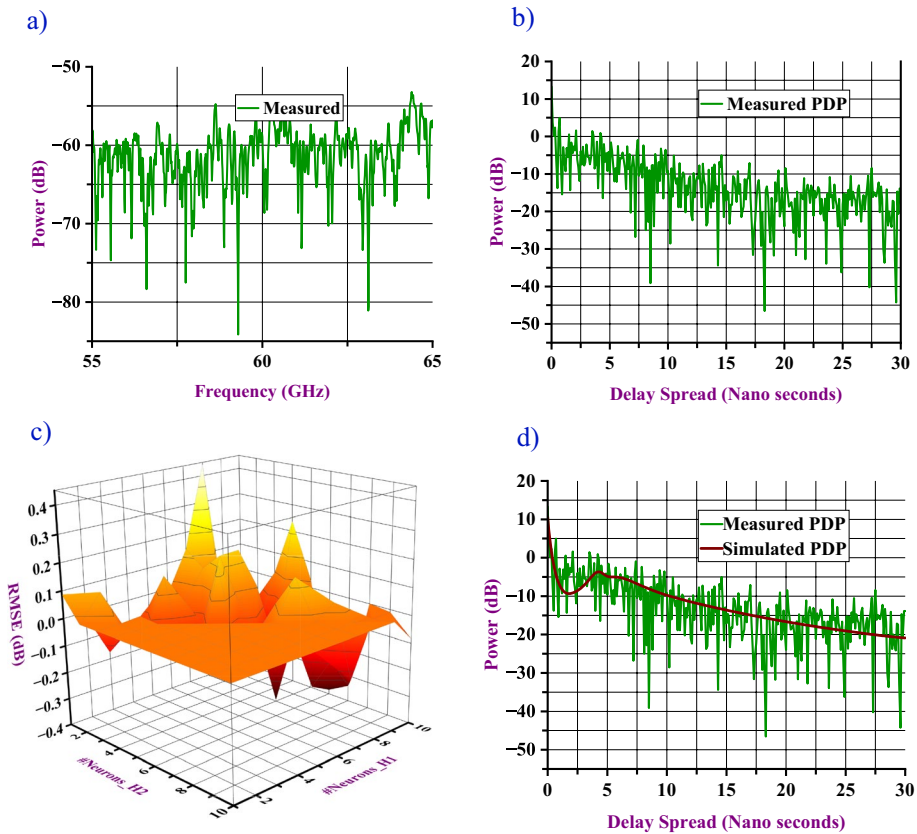


Fig. 6 Direct PDP generation

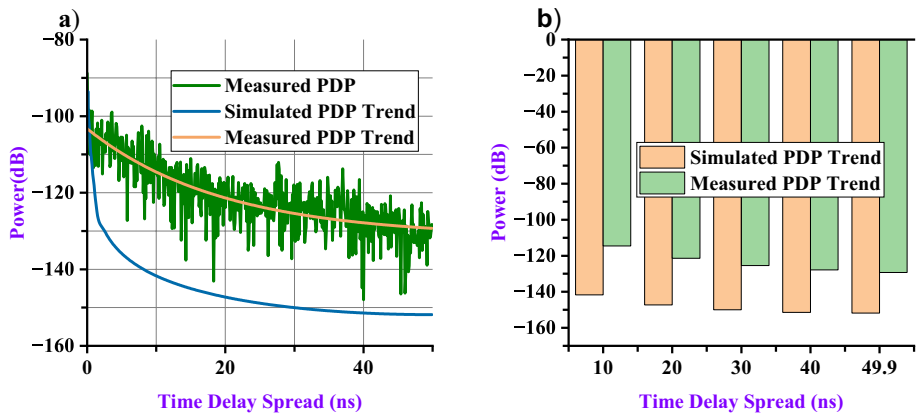


Fig. 7 Tapped delay line analysis for indirect method

The PDP sequence obtained from such multipath channels depicts the time average of tap gains at corresponding tap delays.

As evident from Figs. 8a and 9a, the average trend for measured PDP closely followed the simulated PDP trend for the direct method for PDP generation. On the other hand, we have to note that the effect of the DC offset requirement in Fig. 5 is also shown in Fig. 7 while obtaining the TDL model. When we compared the averaged PDP trend for

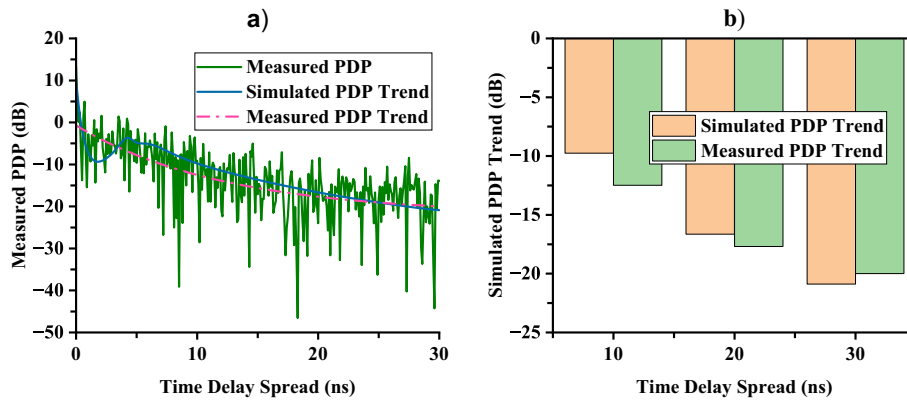


Fig. 8 Tapped delay line analysis for direct method in bus

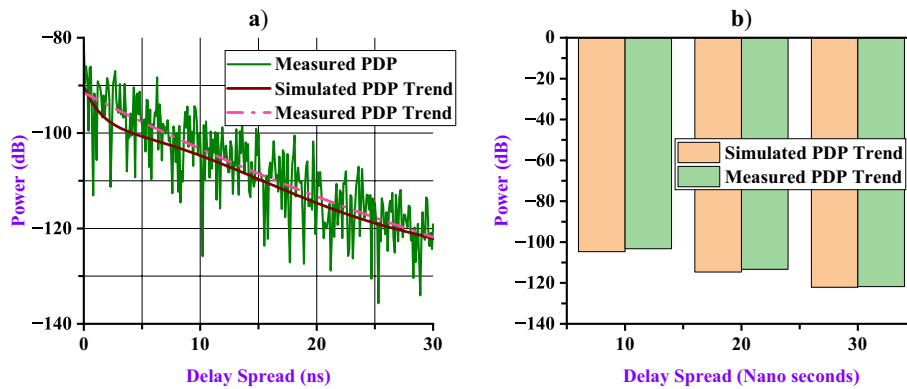


Fig. 9 Tapped delay line analysis for direct method in car

measured values at different tap delays and compared with sampled simulated PDPs, we found that the difference between the tap gains for average measured PDP and simulated PDP is relatively low (Figs. 8b, 9b). Thus, the simulated PDP can replace an average trend of measured PDP.

4.3 Sources of errors

Intra-vehicular scenarios are highly clustered and complex environments. Application of ANN (or any other ML or DL algorithms) in such environments is prone to many errors [32]. For example, the presence or absence of a line-of-sight(LOS) component dramatically influences the performance of ANN models [31]. The higher number of LOS components means more accurate the ANN-based models. Similarly, distance or frequency variations affect the ANN model’s performance. It has been found that ANN models are prone to errors when the receiver is in the vicinity of the transmitter [38]. Also, small-scale fading affects the accuracy of the ANN model [39] for a higher frequency.

4.4 Understanding the errors

As discussed earlier in the section, generating channel characteristics synthetically using ANN algorithms is prone to errors due to the complex and cluttered environment.

Table 1 Error Metrics measured and simulated PDPs

Parameter	BUS			CAR	
	1.47m	5.12m	8.18m	1.48m	2.08m
NRMSE	0.15	0.16	0.66	0.06	0.27
MSE	0.8	0.64	4.54	0.23	5.47
MAE	0.66	0.71	1.88	0.42	2.06

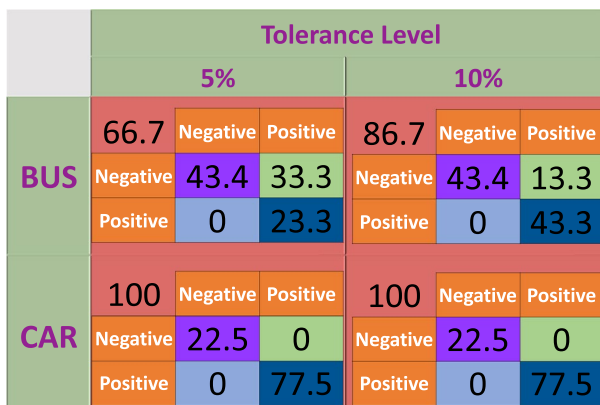


Fig. 10 Tapped delay line analysis for direct method

Thus, we analysed synthetic channel measurements with measured channel measurements. Table 1 shows the NRMSE, MAE and MSE error metrics for the varying distance between transmitter and receiver.

4.5 Sensitivity analysis

The TDL samples are compared with synthetic PDP samples obtained from the direct method for PDP generation with error tolerance levels of 5% and 10%. From the results, we obtain a 2 * 2 confusion matrix. The true positive values indicate the synthetic value is greater than or equal to the TDL value and is within the tolerance limit, whereas true negative indicates the synthetic value is less than the TDL value and within the tolerance level. Similarly, a false positive is when the synthetic PDP value is greater than the TDL value and above the tolerance limit, and a false negative indicates a PDP value less than the TDP value and lesser than the tolerance limit.

From Fig. 10, it is clear that due to a more complex channel environment and greater distance, the MLP channel model for the bus is having lesser accuracy compared to that of the car.

5 Conclusion

This article proposed a feedforward MLP-based ANN framework for a 60-GHz wireless communication link inside a bus and a car. The comprehensive study of frequency-domain channel sounding for mmWave IV measurement campaigns led to the development of simulated PDP using dynamic channel parameters. The highly similar trends of measured and simulated PDPs support that for IVC, PDPs can be

synthetically generated using MLP. Our claim was further supported by the results of the goodness of fit parameters. The accuracy of the MLP model was calculated using a confusion matrix between the simulated PDP trend and the time-averaged tap delay gains with an error tolerance of 5% and 10%. In the case of the bus, the model achieved an accuracy of 66.7% and 86.7% for 5% and 10% tolerances, respectively. In the case of car, the model achieved the target accuracy of 100% for 5% and 10% error tolerance. This indicates that the synthetically generated PDPs from the proposed MLP-based model can replace a measurement-based TDP model when the actual IV channel-sounding data are not available.

Abbreviations

mmWave	Millimetre Wave
CTF	Channel Transfer Function
PDP	Power Delay Profile
IVC	Intra-Vehicular Communication
IV	Intra-Vehicular
ANN	Artificial Neural Network
GHz	Giga Hertz
TDL	Tapped Delay Line
AP	Access Point
V2I	Vehicle to Infrastructure
DC	Direct Current
PA	Power Amplifier
MHz	Mega Hertz
dBm	Decibel–Milliwatts
OWGA	Open Waveguide Antenna
SIW SA	Substrate-Integrated Waveguide Slot Antenna
GPIO	General-Purpose Interface Bus
DL	Deep Learning
MLP	Multi-Layer Perceptron
VNA	Vector Network Analyser
ML	Machine Learning
MSE	Mean Square Error
MAE	Mean Absolute Error
RMSE	Root Mean Square Error
HVAC	Heat Ventilation and Air-Conditioning
5G	Fifth generation
Gbps	Giga bit per second
UWB	Ultrawide band
T_x-R_x	Transmitter–receiver
MPC	Multipath component
MLP	Multilayer perceptron
RT	Ray Tracing
DRL	Deep reinforcement learning
LSTM	Long short-term memory
CIR	Channel impulse response
IFFT	Inverse fast Fourier transform

Acknowledgements

Not applicable.

Author contributions

RS conceptualised the work, performed simulations, and derived comparatives. ANS wrote the ANN algorithm and jointly wrote the manuscript with RS. AC supervised the project. JK, CZ, TM, and AP are the foreign collaborators responsible for obtaining measured datasets along with AC.

Funding

This work was developed within a framework of the research grants: Project No. 23-04304 L sponsored by the Czech Science Foundation, MubaMilWave no. 2021/43/I/ST7/03294 sponsored by the National Science Center (NCN) Poland under the OPUS call in the Weave programme, and Grant No. UGB/22-863/2023/WAT sponsored by the Military University of Technology.

Data availability

The data supporting this study's findings are available from the corresponding author upon reasonable request.

Declarations

Competing interests

The authors declare that they have no competing interests.

Received: 22 July 2022 Accepted: 1 June 2023

Published online: 10 June 2023

References

1. J. O'Halloran, 5G drives connected car surge. *Computer Weekly* (2023). <https://www.computerweekly.com/news/365533698/5G-drives-connected-car-surge>
2. P. Hunter. Connected cars surge as 5G enters the scene. Rethink Technology Research, RAN Research, Connected Car Forecast (2023). <https://rethinkresearch.biz/wp-content/uploads/2023/03/Connected-Car-Forecast-Executive-Summary-PDF-a5a25.pdf>
3. M. Ahmed, C.U. Saraydar, T. ElBatt, J. Yin, T. Talty, M. Ames, Intra-vehicular wireless networks. in *2007 IEEE Globecom Workshops*, pp. 1–9 (2007)
4. J. Blumenstein, A. Prokes, A. Chandra, T. Mikulasek, R. Marsalek, T. Zemen, C. Mecklenbräuker, In-vehicle channel measurement, characterization, and spatial consistency comparison of 30–11 GHz and 55–65 GHz frequency bands. *IEEE Trans. Veh. Technol.* **66**(5), 3526–3537 (2017)
5. A. Chandra, T. Mikulasek, J. Blumenstein, A. Prokes, 60 GHz mmW channel measurements inside a bus, in *2016 8th IFIP International Conference on New Technologies, Mobility and Security (NTMS)*, pp. 1–5 (2016)
6. C. Huang, R. He, B. Ai, A.F. Molisch, B.K. Lau, K. Haneda, B. Liu, C.-X. Wang, M. Yang, C. Oestges, Z. Zhong, Artificial intelligence enabled radio propagation for communications—Part II: Scenario identification and channel modeling. *IEEE Trans. Antennas Propag.* **70**(6), 3955–3969 (2022). <https://doi.org/10.1109/TAP.2022.3149665>
7. D.W. Matolak, A. Chandrasekaran, Aircraft intra-vehicular channel characterization in the 5 GHz band, in *2008 Integrated Communications, Navigation and Surveillance Conference*, pp. 1–6 (2008). <https://doi.org/10.1109/ICNSURV.2008.4559193>
8. J. Pascual-García, L. Rubio, V.M. Rodrigo Peñarrocha, L. Juan-Llácer, J.-M. Molina-García-Pardo, C. Anchis-Borrás, C. Reig, J.(2022). Wireless channel analysis between 25 and 40 GHz in an intra-wagon environment for 5g using a ray-tracing tool. *IEEE Trans. Intell. Transp. Syst.* **23**(12), 24621–24635. <https://doi.org/10.1109/TITS.2022.3199159>
9. K. Guan, B. Peng, D. He, J.M. Eckhardt, S. Rey, B. Ai, Z. Zhong, T. Kürner, Channel characterization for intra-wagon communication at 60 and 300 GHz bands. *IEEE Trans. Veh. Technol.* **68**(6), 5193–5207 (2019). <https://doi.org/10.1109/TVT.2019.2907606>
10. L. Rubio, V.M. Rodrigo Peñarrocha, J.-M. Molina-García-Pardo, L. Juan-Llácer, J. Pascual-García, J. Reig, C. Sanchis-Borrás, Millimeter wave channel measurements in an intra-wagon environment. *IEEE Trans. Veh. Technol.* **68**(12), 12427–12431 (2019). <https://doi.org/10.1109/TVT.2019.2947205>
11. K. Guan, B. Ai, D. He, F. Zhu, H. Yi, J. Dou, Z. Zhong, Channel sounding and ray tracing for thz channel characterization, in *2020 13th UK-Europe-China Workshop on Millimetre-Waves and Terahertz Technologies (UCMMT)*, pp. 1–3 (2020). <https://doi.org/10.1109/UCMMT49983.2020.9295992>
12. V. Semkin, A. Ponomarenko-Timofeev, A. Karttunen, O. Galinina, S. Andreev, Y. Koucheryavy, Path loss characterization for intra-vehicle wearable deployments at 60 GHz, in *2019 13th European Conference on Antennas and Propagation (EuCAP)*, pp. 1–4 (2019)
13. A. Chandra, A.U. Rahman, U. Ghosh, J.A. García-Naya, A. Prokeš, J. Blumenstein, C.F. Mecklenbräuker, 60-GHz millimeter-wave propagation inside bus: measurement, modeling, simulation, and performance analysis. *IEEE Access* **7**, 97815–97826 (2019)
14. A.U. Rahman, U. Ghosh, A. Chandra, A. Prokes, Channel modelling for 60 GHz mmwave communication inside bus, in *2018 IEEE Vehicular Networking Conference (VNC)*, pp. 1–6 (2018)
15. A. Chandra, A. Prokeš, T. Mikulášek, J. Blumenstein, P. Kukolev, T. Zemen, C.F. Mecklenbräuker, Frequency-domain in-vehicle uwb channel modeling. *IEEE Trans. Veh. Technol.* **65**(6), 3929–3940 (2016). <https://doi.org/10.1109/TVT.2016.2550626>
16. L. Liu, Y. Wang, N. Zhang, Y. Zhang, UWB channel measurement and modeling for the intra-vehicle environments, in *2010 IEEE 12th International Conference on Communication Technology*, pp. 381–384 (2010). <https://doi.org/10.1109/ICCT.2010.5688815>
17. J. Blumenstein, T. Mikulasek, A. Prokes, T. Zemen, C. Mecklenbrauker, Intra-vehicular path loss comparison of UWB channel for 3–11 GHz and 55–65 GHz, in *2015 IEEE International Conference on Ubiquitous Wireless Broadband (ICUWB)*, pp. 1–4 (2015). <https://doi.org/10.1109/ICUWB.2015.7324466>
18. J. Blumenstein, A. Prokes, A. Chandra, T. Mikulasek, R. Marsalek, T. Zemen, C. Mecklenbräuker, In-vehicle channel measurement, characterization, and spatial consistency comparison of 30–11 GHz and 55–65 GHz frequency bands. *IEEE Trans. Veh. Technol.* **66**(5), 3526–3537 (2017). <https://doi.org/10.1109/TVT.2016.2600101>
19. J. Vychodil, J. Blumenstein, T. Mikulasek, A. Prokes, V. Derbek, Measurement of in-vehicle channel—feasibility of ranging in UWB and MMW band, in *2014 International Conference on Connected Vehicles and Expo (ICCVE)*, pp. 695–698 (2014). <https://doi.org/10.1109/ICCVE.2014.7297639>
20. A. Prokes, T. Mikulasek, J. Blumenstein, C.F. Mecklenbrauker, T. Zemen, Intra-vehicle ranging in ultra-wide and millimeter wave bands, in *2015 IEEE Asia Pacific Conference on Wireless and Mobile (APWiMob)*, pp. 246–250 (2015). <https://doi.org/10.1109/APWiMob.2015.7374969>
21. M. Schack, M. Jacob, T. Kiirner, Comparison of in-car UWB and 60 GHz channel measurements, in *Proceedings of the Fourth European Conference on Antennas and Propagation*, pp. 1–5 (2010)

22. S.M. Aldossari, K.-C. Chen, Machine learning for wireless communication channel modeling: an overview. *Wirel. Personal Commun.* **106**(1), 41–70 (2019). <https://doi.org/10.1007/s11277-019-06275-4>
23. L. Yin, R. Yang, Y. Yao, Channel sounding and scene classification of indoor 6g millimeter wave channel based on machine learning. *Electronics* **10**(7) (2021). <https://doi.org/10.3390/electronics10070843>
24. P. Zhang, C. Yi, H. Wang, Machine-learning-assisted modeling of millimeter-wave channels, in *2021 IEEE International Symposium on Antennas and Propagation and USNC-URSI Radio Science Meeting (APS/URSI)*, pp. 233–234 (2021). <https://doi.org/10.1109/APS/URSI47566.2021.9704405>
25. Y. Tian, M. Khishe, R. Karimi, E. Hashemzadeh, O. Pakdel Azar, Underwater image detection and recognition using radial basis function neural networks and chimp optimization algorithm. *Circuits Syst. Signal Process.* (2023)
26. M. Kamalipour, H. Agahi, M. Khishe, A. Mahmoodzadeh, Variable-length deep convolutional neural networks by internet protocol chimp optimization algorithm for underwater micro-target classification. *Iran. J. Mar. Technol.* **9**(4), 1–18 (2022)
27. M. Khishe, E. Ebrahimi, A. Goldani, Designing a sonar system with the ability of classifying active and passive acoustic targets based on the evolutionary neural network. *J. Adv. Defense Sci. Technol.* **11**(2), 191–203 (2020)
28. A. Saffari, M. Khishe, M. Mohammadi, A. Hussein Mohammed, S. Rashidi, DCNN-fuzzyWOA: artificial intelligence solution for automatic detection of covid-19 using X-ray images. *Comput. Intell. Neurosci.* (2022)
29. H. Kosarirad, M. Ghasempour Nejati, A. Saffari, M. Khishe, M. Mohammadi, Feature selection and training multilayer perceptron neural networks using grasshopper optimization algorithm for design optimal classifier of big data sonar. *J. Sensors* **2022**, 9620555 (2022)
30. C. Huang, R. He, B. Ai, A.F. Molisch, B.K. Lau, K. Haneda, B. Liu, C.-X. Wang, M. Yang, C. Oestges, Z. Zhong, Artificial intelligence enabled radio propagation for communications—part I: channel characterization and antenna-channel optimization. *IEEE Trans. Antennas Propag.* **70**(6), 3939–3954 (2022). <https://doi.org/10.1109/TAP.2022.3149663>
31. A. Seretis, X. Zhang, K. Zeng, C.D. Sarris, Artificial neural network models for radiowave propagation in tunnels. *IET Microwaves Antennas Propag.* **14**(11), 1198–1208 (2020)
32. A. Seretis, C.D. Sarris, An overview of machine learning techniques for radiowave propagation modeling. *IEEE Trans. Antennas Propag.* **70**(6), 3970–3985 (2022)
33. A. Seretis, C.D. Sarris, Toward physics-based generalizable convolutional neural network models for indoor propagation. *IEEE Trans. Antennas Propag.* **70**(6), 4112–4126 (2022)
34. T. Xiao, C. Chen, S. Wan, Mobile-edge-platooning cloud: a lightweight cloud in vehicular networks. *IEEE Wirel. Commun.* **29**(3), 87–94 (2022)
35. J. Huang, H. Gao, S. Wan, Y. Chen, Aol-aware energy control and computation offloading for industrial IoT. *Future Gener. Comput. Syst.* **139**, 29–37 (2023)
36. C. Chen, J. Jiang, Y. Zhou, N. Lv, X. Liang, S. Wan, An edge intelligence empowered flooding process prediction using internet of things in smart city. *J. Parallel Distrib. Comput.* **165**, 66–78 (2022)
37. K. Hornik, M. Stinchcombe, H. White, Multilayer feedforward networks are universal approximators. *Neural Netw.* **2**(5), 359–366 (1989). [https://doi.org/10.1016/0893-6080\(89\)90020-8](https://doi.org/10.1016/0893-6080(89)90020-8)
38. M. Ayadi, A.B. Zineb, S. Tabbane, A uhf path loss model using learning machine for heterogeneous networks. *IEEE Trans. Antennas Propag.* **65**(7), 3675–3683 (2017)
39. I. Popescu, I. Nafomita, P. Constantinou, A. Kanatas, N. Moraitis, Neural networks applications for the prediction of propagation path loss in urban environments. in *IEEE VTS 53rd Vehicular Technology Conference, Spring 2001. Proceedings (Cat. No. 01CH37202)*, vol. 1, pp. 387–391 (2001). IEEE

Publisher's Note

Springer Nature remains neutral with regard to jurisdictional claims in published maps and institutional affiliations.

Submit your manuscript to a SpringerOpen[®] journal and benefit from:

- Convenient online submission
- Rigorous peer review
- Open access: articles freely available online
- High visibility within the field
- Retaining the copyright to your article

Submit your next manuscript at ► [springeropen.com](https://www.springeropen.com)
